3D and 4D Space-Time Grids for Electromagnetic Field Analysis Using Finite Integration Method

Tetsuji Matsuo and Takeshi Mifune

Graduate School of Engineering, Kyoto University, Japan

1 Introduction

The finite integration (FI) method [1]-[4] has been studied to realize time-domain electromagnetic field computation using unstructured spatial grid. However, similarly to the FDTD method, the FI method uses a uniform time-step, which is restricted by the CFL condition based on the smallest spatial grid size. Previous works [5], [6] introduced a space-time FI method that achieves non-uniform time-steps naturally on 3D and 4D space-time grids with 2D and 3D space. However, it was found that a rough construction of space-time grid results in computational inaccuracy because of unphysical wave-reflection. Ref. [7] proposed improved 3D and 4D space-time grids for accurate electromagnetic wave computation. This study proposes another improved FI method.

2 Finite Integration Method on a Space–Time Grid

The coordinate system is denoted by:

$$(ct, x, y, z) = (x^0, x^1, x^2, x^3) \tag{1}$$

where $c = 1 / \sqrt{(\varepsilon_0 \mu_0)}$, and ε_0 and μ_0 are the electric and magnetic constants. The Maxwell equations are given as :

$$\mathrm{d}F = 0\ ,\ \mathrm{d}G = J \tag{2}$$

$$F = -\Sigma_{i=1}^{3} E_i \mathrm{d}x^0 \mathrm{d}x^i + \Sigma_{j=1}^{3} \mathfrak{B}_j \mathrm{d}x^k \mathrm{d}x^l,$$

$$G = \Sigma_{i=1}^{3} H_i \mathrm{d}x^0 \mathrm{d}x^i + \Sigma_{j=1}^{3} \mathfrak{D}_j \mathrm{d}x^k \mathrm{d}x^l,$$

$$J = c\rho \mathrm{d}x^1 \mathrm{d}x^2 \mathrm{d}x^3 - \Sigma_{j=1}^{3} J_j \mathrm{d}x^0 \mathrm{d}x^k \mathrm{d}x^l \tag{3}$$

where $(\mathfrak{B}_1, \mathfrak{B}_2, \mathfrak{B}_3) = c\boldsymbol{B}$, $(\mathfrak{D}_1, \mathfrak{D}_2, \mathfrak{D}_3) = c\boldsymbol{D}$, and ρ is the electric charge density; (j, k, l) is a cyclic permutation of (1, 2, 3).

The integrated form of (3) is given as:

$$\oint_{\partial\Omega_p} F = 0\ ,\ \oint_{\partial\Omega_d} G = \int_{\Omega_d} J \tag{4}$$

where Ω_p and Ω_d are hypersurfaces in space-time; their boundaries $\partial\Omega_p$ and $\partial\Omega_d$ are represented by the faces of primal and dual grids in the FI method. The electromagnetic variables are defined in the FI method as:

$$f = \int_{S_p} F\ ,\ g = \int_{S_d} G, \tag{5}$$

where S_p and S_d are the faces of primal and dual grids.

The Hodge dual grid [6] is used to express the constitutive equation simply as:

$$\int_{S_d} c_r \mathrm{d}x^0 \mathrm{d}x^j \,/\, \int_{S_p} \mathrm{d}x^k \mathrm{d}x^l = -\int_{S_d} \mathrm{d}x^k \mathrm{d}x^l \,/\, \int_{S_p} c_r \mathrm{d}x^0 \mathrm{d}x^j = a \tag{6}$$

$$c_r = 1 / \sqrt{(\varepsilon_r \mu_r)} \tag{7}$$

where a is a constant determined for each pair of S_p and S_d; (j, k, l) is a cyclic permutations of (1, 2, 3); ε_r and μ_r are the specific permittivity and permeability. Thereby,

$$f = Zg / a \tag{8}$$

where $Z = \sqrt{(\mu_r \mu_0 / \varepsilon_r \varepsilon_0)}$ is the impedance.

3 3D Space–Time Grid with 2D Space

Figure 1 illustrates space-time grids where domains (I) and (II) have uniform time-steps Δx^0 and $\Delta x^0/2$, respectively; domain (III) is the connecting domain. The grid shown in Fig. 1(a) was proposed in [5] that causes unphysical wave-reflection because of spatial irregularity as reported in [5]. This paper proposes the grid shown in Fig. 1(b) to suppress the unphysical reflection. The former and latter grids are called type A and type B in this article.

Type B grid has dual edges that are not orthogonal to corresponding primal faces as shown in Fig. 2. This study examines two types of constitutive relations described by Eqs. (9) and (10).

$$e_{xi} = \varepsilon_r \varepsilon_0 \, d_{xi} / \Delta l\ ,\ e_{yi} = \varepsilon_r \varepsilon_0 \, d_{yi} / \Delta l \ \ (i = 1, 2) \tag{9}$$

$$e_{x1} = \varepsilon_r \varepsilon_0 \, (d_{x1} + d_{xy}/2)\ ,\ e_{y1} = \varepsilon_r \varepsilon_0 \, (d_{y1} - d_{xy}/2)\ ,$$

$$e_{x2} = \varepsilon_r \varepsilon_0 \, [\Delta l \, d_{x2} - (1 - \Delta l) \, d_{y2}] \,/\, (1 - 2\Delta l)\ ,$$

$$e_{y2} = \varepsilon_r \varepsilon_0 \, [\Delta l \, d_{y2} - (1 - \Delta l) \, d_{x2}] \,/\, (1 - 2\Delta l) \tag{10}$$

where d and e are the electric flux and the integration of electric field given by Eq. (5), respectively. Equation (10) gives more accurate approximation of constitutive relation than Eq. (9).

Fig. 3 portrays distributions of discrepancy $\Delta\mathfrak{B}_3$ between $\mathfrak{B}_3$ obtained in the same way as in [8] by the FDTD method and the FI method with the two space-time grids. The type A grid yields numerical error whereas the numerical error is suppressed by the type B grid with Eq. (10) type relation.

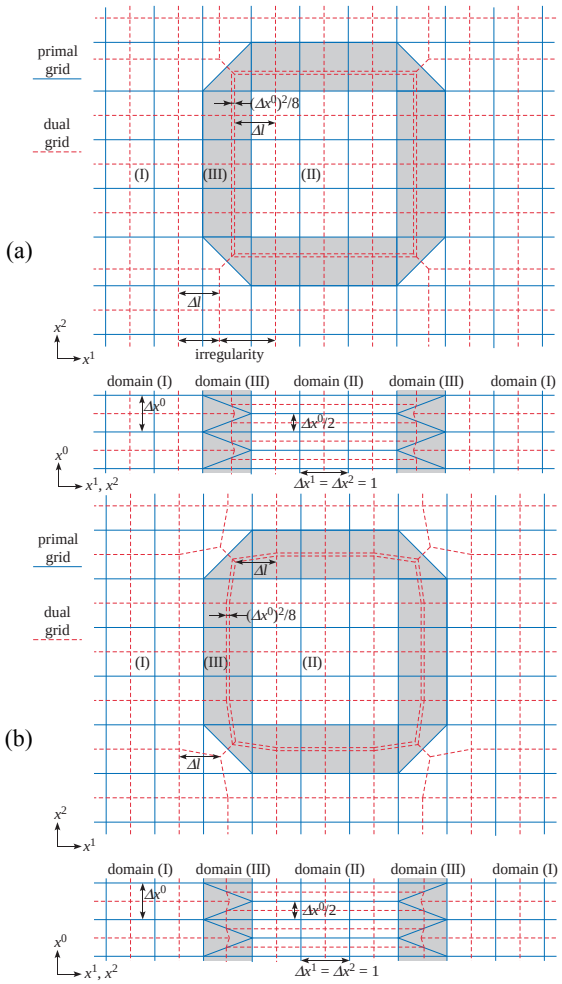

Fig. 1. Space-time grids: (a) type A and (b) type B.

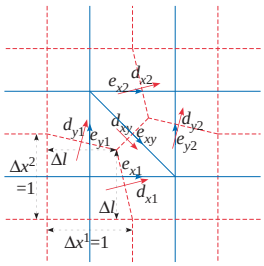

Fig. 2. Coner of domain (III).

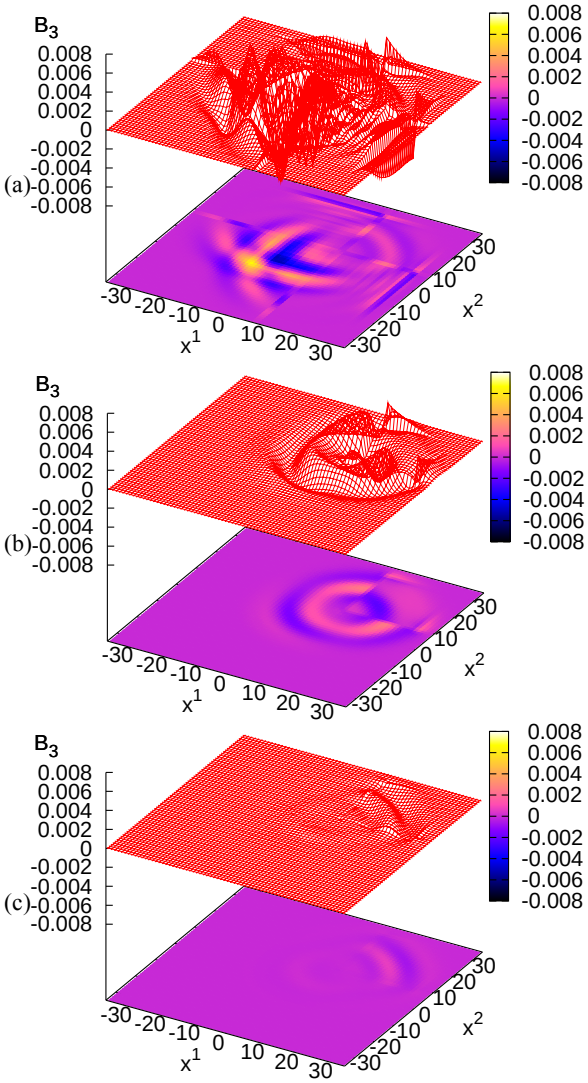

Fig. 3. Discrepancy of $\mathfrak{B}_3$ between space-time FI method and FDTD method: (a) type A grid, (b) type B grid with Eq. (9) relation, and (c) type B grid with Eq. (10) relation.

4 4D Space–Time Grid with 3D Space

Figure 4 illustrates 4D space-time grids of type B at the corner of domain (III). A wave propagation is simulated similarly to [6], where electromagnetic wave is scattered by a cubic pore with $\varepsilon_r = 1$ surrounded by dielectric with $\varepsilon_r = 5$. Figures 5(b)(c) and (d) portray distributions of $\mathfrak{B}_3$ given by the space-time FI method with type A and B grids. For comparison, Fig. 5(a) depicts the distribution obtained using the FDTD method with the same uniform spatial grid and time-step as in domain (II), which is restricted by the smallest permittivity. The FDTD method requires about two times as much computation time as the space-time FI method. The type B grid with Eq. (10) type relation yields more accurate distribution than type A. The numerical instability is not observed even after $x^0 = 10^5 \Delta x^0$.

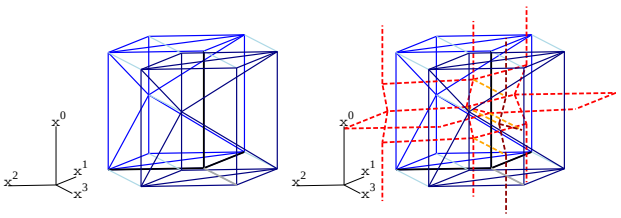

Fig. 4. Space-time grid of type B where solid and dashed lines represent primal and dual grids: (left) primal grid, (right) primal and dual grids.

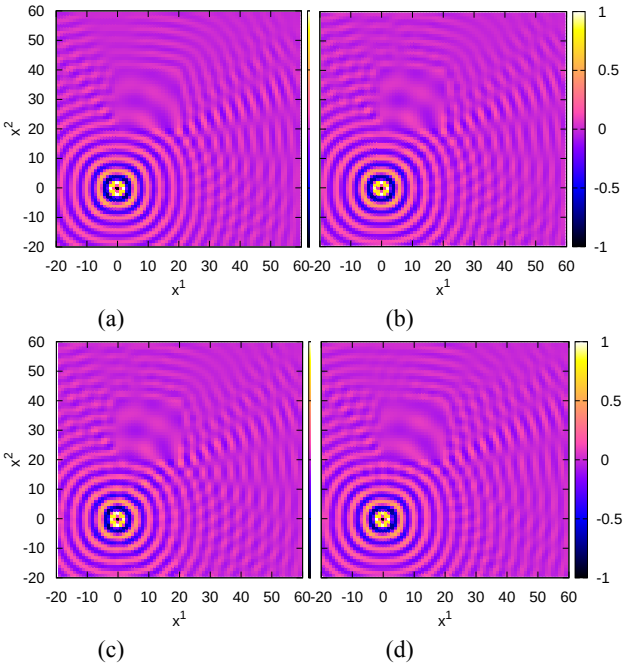

Fig. 5. Scattering of $\mathfrak{B}_3$: (a) FDTD method, (b) type A grid, (c) type B grid with Eq. (9) relation, and type B grid with Eq. (10) relation.

References

[1] T. Weiland, Time domain electromagnetic field computation with finite difference methods, Int. J. Numer. Model., vol. 9, pp. 295-319, 1996.

[2] I. E. Lager, E. Tonti, A.T. de Hoop, G. Mur, and M. Marrone, Finite formulation and domain-integrated field relations in electromagnetics - a synthesis, IEEE Trans. Magn., vol. 39, pp. 1199-1202, May 2003

[3] P. Alotto, A. De Cian, and G. Molinari, A time-domain 3-D full-Maxwell solver based on the cell method, IEEE Trans. Magn., vol. 42, pp. 799-802, Apr. 2006.

[4] L. Codecasa and M. Politi, Explicit, consistent, and conditionally stable extension of FD-TD to tetrahedral grids by FIT, IEEE Trans. Magn., vol. 44, pp. 1258-1261, June 2008.

[5] T. Matsuo, Electromagnetic field computation using space-time grid and finite integration method, IEEE Trans. Magn., vol. 46, pp. 3241-3244, Aug. 2010.

[6] T. Matsuo, Space-time finite integration method for electromagnetic field computation, IEEE Trans. Magn.,vol. 47, pp. 1530-1533, May 2011.

[7] T. Matsuo, S. Shimizu, and, T. Mifune, 3D and 4D space-time grids for electromagnetic wave computation using finite integration method, 2012 APS-URSI, 362.3, 2012.

[8] S. Shimizu, T. Mifune, and, T. Matsuo, Space-time grids for electromagnetic field computation using finite integration method, 2011 APS-URSI, pp. 2346 – 2349, 2011.